Available online at www.sciencedirect.com
ScienceDirect
Biochemical and Biophysical Research Communications 367 (2008) 60–66
BBRC
www.elsevier.com/locate/ybbrc

A molecular modeling approach defines a new group of Nodulin 26-like aquaporins in plants

Pierre Rougé *, Annick Barre

Surfaces Cellulaires et Signalisation chez les Végétaux, UMR Université Paul Sabatier-CNRS 5546, 24 Chemin de Borde Rouge, 31326 Castanet Tolosan, France

Received 6 December 2007
Available online 26 December 2007

Abstract

The three-dimensional models built for the Nod26-like aquaporins all exhibit the typical α-helical fold of other aquaporins containing the two ar/R and NPA constriction filters along the central water channel. Besides these structural homologies, they readily differ with respect to the amino acid residues forming the ar/R selective filter. According to these discrepancies in both the hydrophilicity and pore size of the ar/R filter, Nod26-like aquaporins can be distributed in three subgroups corresponding to NIP-1, NIP-II and a third subgroup of Nod26-like aquaporins exhibiting a highly hydrophilic and widely open filter. However, all Nod26-like aquaporins display a bipartite distribution of electrostatic charges along the water channel with an electropositive extracellular vestibular portion followed by an electronegative cytosolic vestibular portion. The specific transport of water, non-ionic solutes (glycerol, urea, ammoniac), ions (NH_4^+) and gas (NH_3) across the Nod26-like obviously depends on the electrostatic and conformational properties of their central water channel.

Keywords: Nodulin 26; Aquaporin; Three-dimensional model; Legume plants; Nitrogen-fixation symbiosis

Plant channel proteins known as aquaporins (AQPs) consist of a family of membrane major intrinsic α-helical proteins (MIPs) that have been classified in three subroups according to their transport facilities: (1) aquaporins or AQPs specific for water transport, (2) glycerol facilitators or GlpFs specific for small carbohydrates (glycerol) transport and, (3) aquaglyceroporins or AQP3s which insure the transport of both water and small non-ionic solute molecules [1]. With respect to their sequence homologies and sub-cellular localization, four subgroups have been identified: (1) the tonoplast intrinsic proteins or TIPs, (2) the plasma membrane intrinsic proteins or PIPs, (3) the Nodulin26-like intrinsic membrane proteins or NIPs and, (4) the small basic intrinsic proteins or SIPs [2–5]. Aquaporins identified as late-nodulins or nodulin26 proteins were first characterized in soybean [6] and subsequently in other rhizobia-symbiotic legumes [7,8]. These Nod26-like aquaporins are located in the symbiosome or peribacteroid membrane of the nitrogen-fixing cells in functional nodules [9] but also occur in non-symbiotic plants, e.g. in *Arabidopsis* [10] and rice [11]. They have been classified in two distinct subgroups of NIP-I and NIP-II according to the amino acids forming the aromatic and arginin selective filter (ar/R region) of their central water channel [12].

As shown from extensive studies essentially performed on the Nod26 aquaporin (GmNod26) from soybean (*Glycine max*) [13,14], the Nod26-like aquaporins correspond to glyceroaquaporins involved in the transport of both water and glycerol across the plasma membrane [15]. They are thus considered as key nodulins responsible for the osmoregulation inside the nodule and contributing to the carbon supply by the host-plant to the bacteroids since fast- and slow-growing *Rhizobium* strains were demonstrated to contain two glycerol-inducible ATP-glycero kinase and glycerophosphate dehydrogenase susceptible to metabolize glycerol as a carbon source [16]. They similarly stimulate the rate of dicarboxylate (malate) uptake

* Corresponding author. Fax: +33 (0)5 62 193502.
E-mail address: rouge@scsv.ups-tlse.fr (P. Rougé).

0006-291X/$ - see front matter © 2007 Elsevier Inc. All rights reserved.
doi:10.1016/j.bbrc.2007.12.079

across the symbiosome membrane upon phosphorylation which are likely to be the major source of carbon supplied to the bacteroids [17]. Other Nod26-like aquaporins from non-legume plants apparently fulfill a similar transport function. However, some experimental results support other possible transport functions towards non-ionic solutes like urea or ammoniac [15,18]. In this respect, CpNod26 from zucchini (*Cucurbita pepo*), was successfully used to complement a yeast mutant defective in the plasma membrane urea transporter Dur3p [19]. Moreover, another proposed function of Nod26-like aquaporins in the facilitated transport of either uncharged NH_3 or NH_4^+ ions across the symbiosome membrane still remains a matter of debate [20]. In this respect, both the size and hydrophilicity of the ar/R filter and the electrostatic properties of the water channel of Nod26-like aquaporins should play a key role to facilitate the flux of NH_3/NH_4^+ across the membrane.

Owing to the structurally conserved character of aquaporins, accurate molecular models have been built for the Nod26-like aquaporins susceptible to reveal the structure–function relationships of this class of transporter proteins and get an insight into their specific functions in plants. With respect to the pore size and hydrophilicity of their ar/R filter Nod26-like aquaporins from the symbiotic chickpea (*Cicer arietinum*) (CaNod26) and the non-symbiotic zucchini (*Cucurbita pepo*) (CpNod26) species readily differ from other Nod26-like aquaporins of the NIP-I and NIP-II subgroups.

Materials and methods

The amino acid sequence alignment was performed with CLUSTAL-X [21] using the Risler's structural matrix for homologies [22]. The Hydrophobic Cluster Analysis (HCA) [23] plot were generated using the HCA server (http://bioserv.rpbs.jussieu.fr) to recognize the structurally conserved regions common to the archeal aquaporin AqpM from *Methanothermobacter marburgensis* [24] and the human aquaporin-1 [25]. According to the percentages of both identity (~22%) and similarity (~60%) legume aquaporins share with other aquaporins, accurate three-dimensional models were built using the X-ray coordinates of AqpM and human aquaporin-1 as templates.

Homology modeling of Nod26-like aquaporins was performed on a Silicon Graphics O2 10000 workstation, using the programs InsightII, Homology and Discover (Accelrys, San Diego CA, USA). The atomic coordinates of both AqpM (PDB code 2F2B) [24] and human aquaporin-1 (PDB code 1H6I) [25] were used as templates. The few steric conflicts resulting from the replacement or the insertion of some residues in the modeled proteins were corrected during the model building procedure using the rotamer library [26] and the search algorithm implemented in the Homology program [27] to maintain proper side-chain orientation. Energy minimization and relaxation of the loop regions were carried out by several cycles of steepest descent using Discover3. A final energy minimization step was performed by ~300 cycles of steepest descent with Discover 3. PROCHECK [28] and the ANOLEA program [29] were used to check the stereochemical quality of the three-dimensional model. Cartoons were drawn and displayed with PyMOL (http://pymol.sourceforge.net.). A clip of 8–16 Å slab across the molecular surface of the modeled aquaporins was used to display the overall shape and size of the transmembrane channel.

Electrostatic potentials were calculated and displayed with GRASP using the parse3 parameters [30]. The solvent probe radius used for molecular surfaces was 1.4 Å and a standard 2.0 Å-Stern layer was used to exclude ions from the molecular surface. The inner and outer dielectric constants applied to the protein and the solvent were, respectively, fixed at 4.0 and 80.0 and the calculations were performed keeping a salt concentration of 0.145 M. Once the electrostatic potentials were mapped on the molecular surface, a clip of 8–16 Å slab was applied across the molecular surface to display the differentially tuned electrostatics regions along the transmembrane channel of the modeled aquaporins.

An unrooted parsimony tree built from the amino acid sequences of different plant aquaporins was displayed with TREEVIEW [31].

Results

Nod26-like aquaporins exhibit a similar three-dimensional structure

The modeled MtNod26 aquaporin from *Medicago truncatula* (AAT35231) exhibits the canonical hourglass-shaped fold of aquaporins built from six α-helices (H1–H6) organized in two symmetrically arrayed tandem repeats, each containing three α-helices (H1–H3 and H4–H6) connected by more or less extended loops, to delineate a core water channel (Fig. 1A). Loops connecting H1–H2, H2–H3, H3–H4, H4–H5 and H5–H6 correspond to LA, LB, LC, LD and LE, respectively (Fig. 1B). Two highly conserved signature motifs Asn139-Pro140-Ser141 (NPA) and Asn250-Pro251-Val250 (NPV) occur in loops LB and LE which contain short α-helices that fold back into the core of the aquaporin to form one of the two major constriction filter occurring along the central water channel (Fig. 1D and E). The second constriction referred to as the aromatic/arginine region (ar/R), is located approximately 8 Å above the NPA region and consists of four amino acid residues from helix H2 (Ala116), helix H5 (Ile238) and loop LE1 + LE2 (Ala247 and Arg251) (Fig. 1C and D). The two cytosolic N- and C-terminal ends of the polypeptide chain contain the putative *N*-glycosylation sites Asn34-Gly-Ser and Asn300-Ala-Ser. Additionally, three putative phosphorylation sites are predicted to occur at Ser174, Thr254 and Ser303 using the NetPhos 2.0 server (http://www.cbs.dtu.dk). Except for Thr254 which belongs to the short α-helical segment of loop LE embedded into the lipid bilayer and is therefore suspected to escape phosphorylation, the two exposed Ser174 and Ser303 occurring in loop LC and the cytosolic C-terminus, respectively, could be actually phosphorylated to participate in the regulation of the water transport through the water channel (Fig. 1B).

Nod26-like aquaporins differ by their ar/R selective filter

Other Nod26-like aquaporins from *Lotus japonicus* (LjLIMP2) (AAF82791), *Glycine max* (GmNod26) (P08995), *Pisum sativum* (PsNod26) (CAB45652), *Cicer arietinum* (CaNod26) (CAG34223) and *Cucurbita pepo* (CpNod26) (CAD67694), were successfully modeled using 2F2B and 1H6I as templates (Fig. 2). In spite of very limited local structural discrepancies, their overall three-

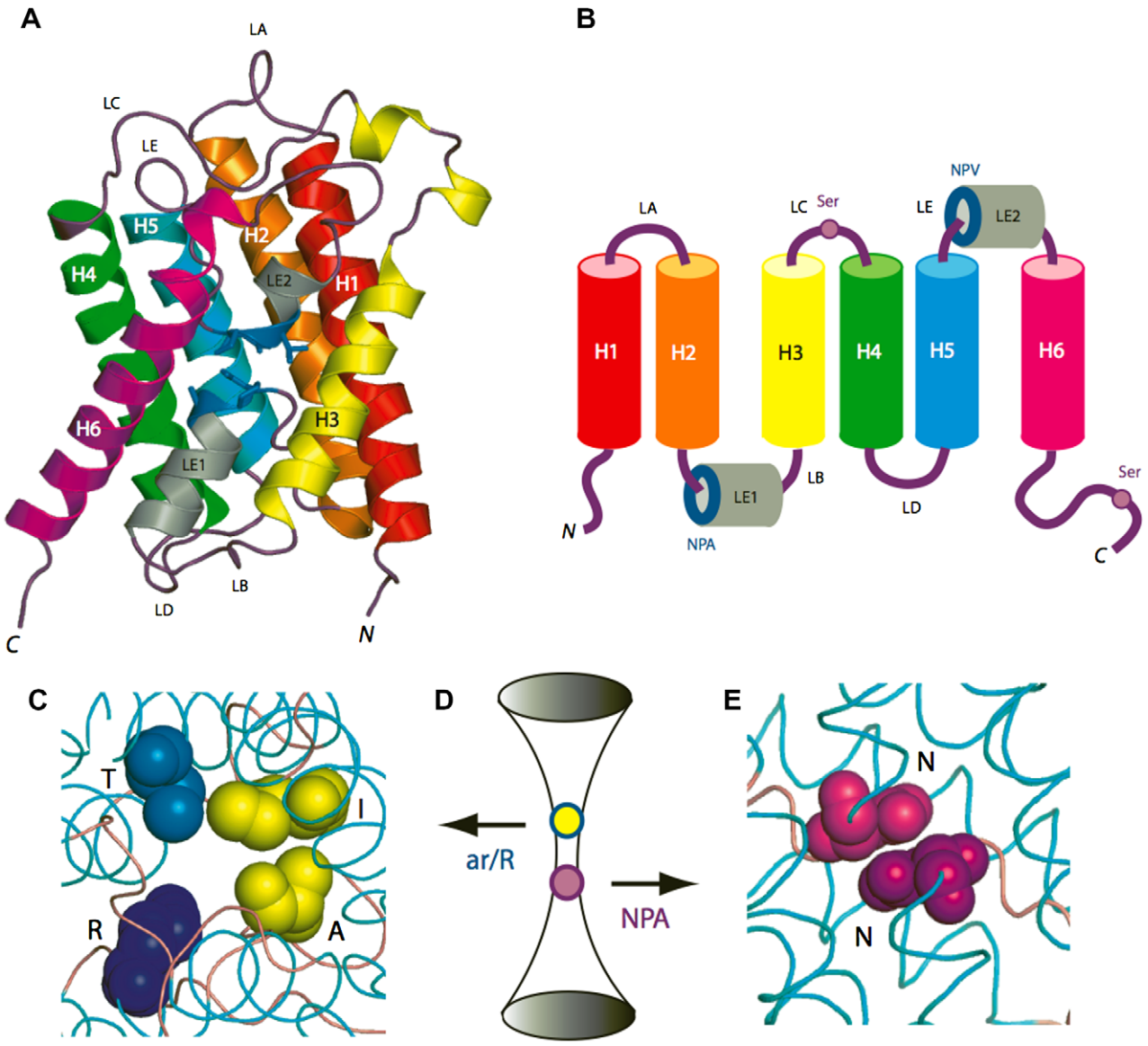

Fig. 1. (A) Ribbon diagram of MtNod26 showing the six α-helices (H1–H6) connected by loops (LA–LE) surrounding the central water channel. Residues forming the two NPA signature motifs are represented in blue sticks. N and C correspond to the N- and C-termini of the polypeptide chain, respectively. (B) Diagram showing the overall organization of the six α-helices (H1–H6) interconnected by loops (LA–LE), that build the Nod26-like aquaporin of *Medicago truncatula*. (C) Spatial organization of residues (CPK representation) forming the ar/R filter of the proximal part (located at the extracellular face) of the water channel. (D) Cartoon showing the localization of the two constriction filters ar/R (yellow/blue) and NPA/NPV (magenta) along the central water channel of MtNod26. Extracellular and cytosolic parts correspond to the upper and lower parts of the channel, respectively. (E) Spatial organization of Asn (N) residues (CPK representation) of the two NPA/NPV signature motifs. (For interpretation of the references to color in this figure legend, the reader is referred to the web version of this paper.)

dimensional fold looks very similar to that of MtNod26. Like in all other plant aquaporins, the water channel exhibits its two constriction filters that play a key role in the selective transport of water and small molecules across the symbiosome membrane. On the basis of the amino acid residues that build the first ar/R filter located at the extracellular moiety of the channel, two subgroups of NIPs have been defined [12]. In GmNod26 and other related aquaporins (PsNod26, LjLIMP2) of the NIP-I subgroup, the four residues correspond to Trp77 (H2), Val196 (H5), Ala206 (LE1) and Arg212 (LE2) (Fig. 3). The hydrophobic residues Trp, Val and Ala, provide a non-polar surface that hydrophobically interacts with the hydrocarbon skeleton of glycerol whereas the Arg residue creates a hydrogen bonding with the hydroxyles of glycerol. In addition, the tiny character of the Val and Ala residues insures a wider aperture for the ar/R filter that should facilitate the transit of glycerol and water molecules across the central water channel. Other Nod26-like aquaporins belonging to the NIP-II subgroup (MtNod26) [(Thr/Ala (H2), Ile (HE), Ala (LE1), Arg (LE2)] essentially differ by the substitution of the bulky Trp residues by a tiny Ala residue whereas the Val residue is replaced by Ile (Fig. 2C). Accordingly, the ar/R filter offers an even wider aperture susceptible to

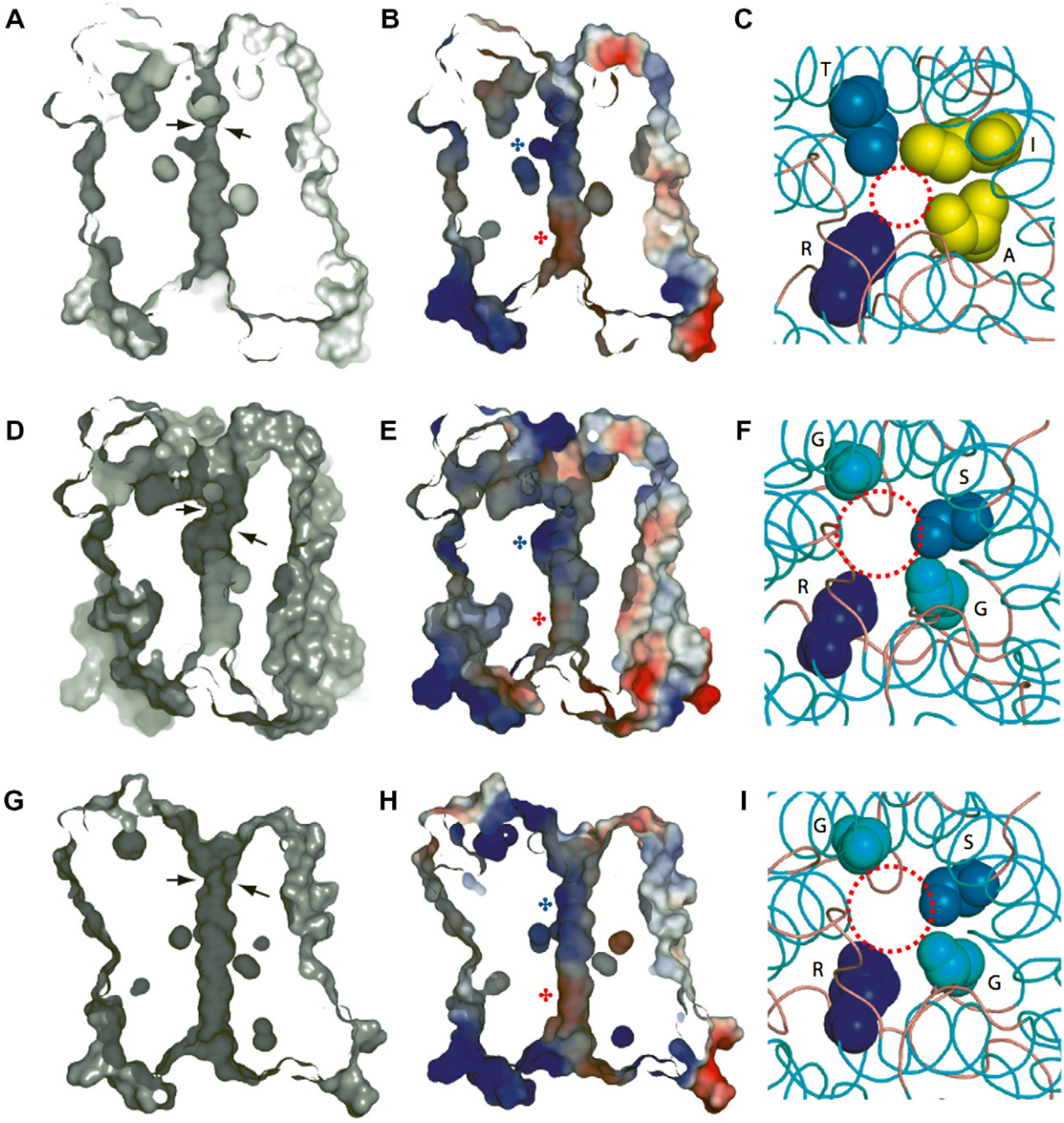

Fig. 2. Clips showing the overall shape of the water channel, electrostatic potentials along the water channel and relative position of residues (represented as space-filling spheres) forming the ar/R constriction filter of the modeled MtNod26 (A–C), CaNod26 (D–F) and CpNod26 (G–I). Black arrows indicate the constriction formed by the ar/R filter. Electropositively (blue) and electronegatively (red) regions are indicated. (For interpretation of the references to color in this figure legend, the reader is referred to the web version of this paper.)

enhance the glycerol and water conductance of the channel. The replacement of Trp by a hydrophilic and smaller Thr residue should create additional hydrogen bond interactions with both the hydroxyls of glycerol and water molecules.

Two Nod26-like aquaporins possess a widely open ar/R filter

The most important discrepancies concern the size and properties of the central water channel that contains the two major constriction filters corresponding to the NPA/NPV signature motif and the ar/R region, respectively (Fig. 2A, D and G). In all of the modeled Nod26-like aquaporins the water channel display opposite electrostatic potentials at both extremities. Their proximal part located at the extracellular face (opposite to the N- and C-terminal side) is preferentially electropositively charged whereas the distal part located at the intracellular face (at the N- and C-terminal side) is electronegatively charged (Fig. 2B, E and H). However, Nod26-like aquaporins from etiolated coty-

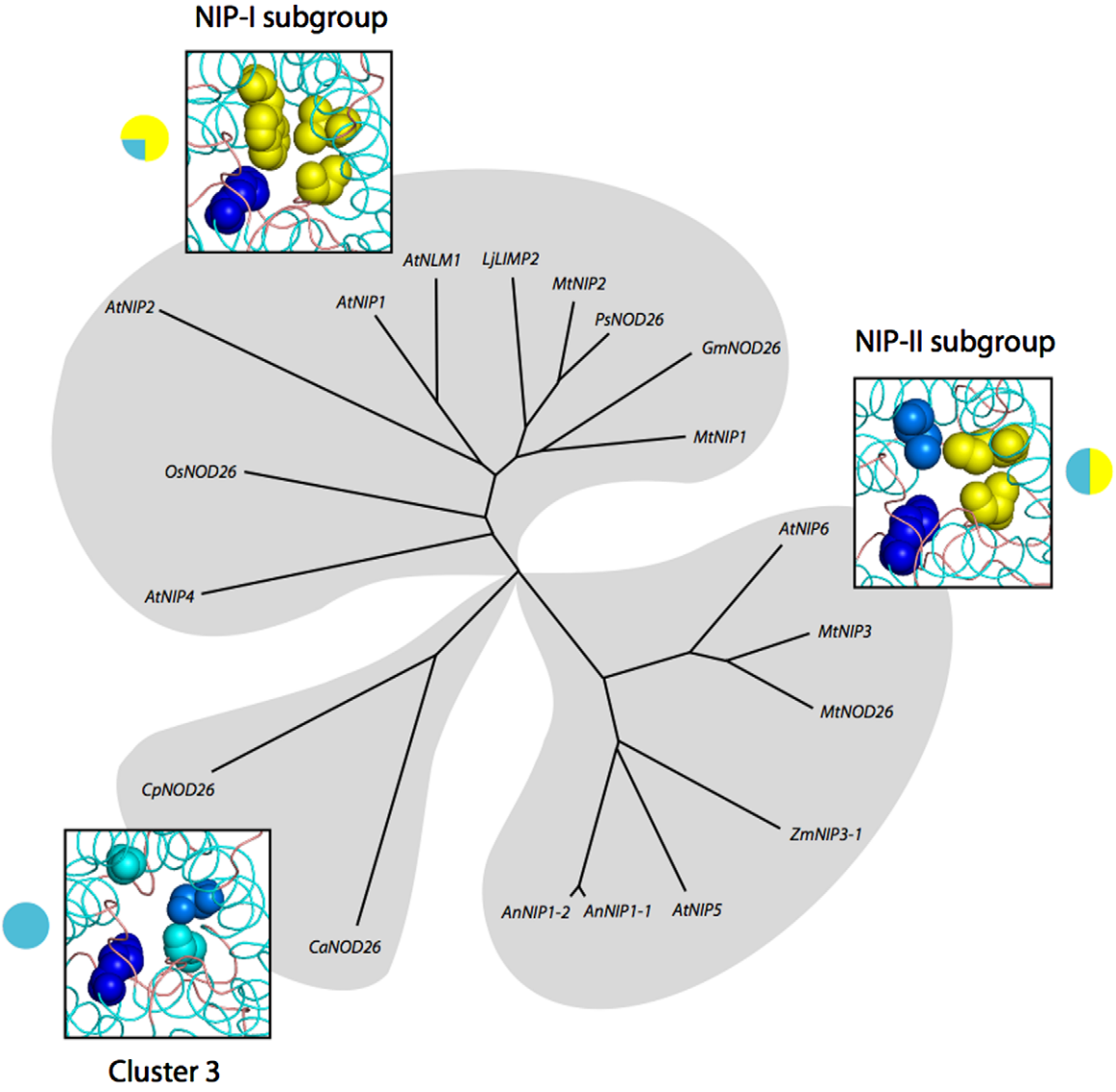

Fig. 3. Parsimony tree built from the amino acid sequences of Nod26-like aquaporins from symbiotic and non-symbiotic plants. Another Nod26-like aquaporin from *Vitis vinifera* [Thr (H2), Ser (H5), Ala (LE1), Arg (LE2)] (CAN83047), which clusters in NIP-II subgroup, is not represented. Ribbon diagrams corresponding to the relative position of amino acid residues forming the ar/R filter are shown opposite to the corresponding clusters. Hydrophobic (yellow) and hydrophilic (blue) residues forming the ar/R filter are shown in the corresponding circles. (For interpretation of the references to color in this figure legend, the reader is referred to the web version of this paper.)

ledons of *Cicer arietinum* seedlings (CaNod26) and *Cucurbita pepo* leaves (CpNod26) readily differ from other aquaporins by a much more hydrophilic ar/R filter [Gly (H2), Ser (H5), Gly (LE1), Arg (LE2)]. Due to the tiny character of the two Gly residues that replace the most bulky Val/Ile and Ala residues in other Nod26-like aquaporins, the ar/R constriction filter is more widely open with a size $\geqslant 6$ Å which readily differs from the narrower ar/R filter ($\leqslant 4$ Å) of other Nod26-like aquaporins (Fig. 2F and I). Interestingly, CaNod26 is apparently involved in the transport of urea since it can complement a yeast mutant defective in the plasma membrane urea transporter Dur3p [19]. Conversely to the ar/R filter, the NPA/NPV filter which consists of the highly conserved twinned triads NPA(S)/NPA(V) of the LE1 and LE2 loops, is readily conserved and displays a similar size in all the modeled Nod26-like aquaporins. Accordingly, the selectivity of the transported solutes across the water channel of Nod26-like aquaporins essentially depends on their ar/R filter.

Phylogenetic clustering of Nod26-like aquaporins

Interestingly, the discrepancies observed in the hydrophobicity and size of the ar/R constriction filter among Nod26-like aquaporins correlate fairly well with their clustering in the parsimony tree built from the available amino acid sequences of Nod26-like aquaporins from both symbiotic and non-symbiotic plants (Fig. 3). The three clusters identified so far correspond to the NIP-I subgroup, the

NIP-II subgroup and a third cluster grouping Nod26-like aquaporins containing a totally hydrophilic and largely open ar/R filter (CaNod26, CpNod26), respectively.

Discussion

The legume Nod26-like channel proteins of the aquaglyceroporin subgroup have been characterized as late nodulins responsible for the transport of both water, small non-ionic solutes (glycerol, formamide) and charged ions (malate) across the symbiosome membrane of symbiotic nitrogen-fixing rhizobia in functional nodules [5]. Nod26-like aquaporins all exhibit a very similar three-dimensional organization consisting of a pseudo-symmetrical tandem repeat of a three α-helical motif forming an outer crown of six α-helices surrounding a central water channel. This molecular organization confers a canonical hourglass shape to plant aquaporins characterized so far, including the divergent SIP class of aquaporins (result not shown).

TIP2 aquaporins from wheat (*Triticum aestivum*) were previously characterized as a new group of NH_3-transporting aquaporins or aquaammoniaporins, which exhibit a specific ar/R signature consisting of the four residues His (H2), Ile (H5), Gly (LE1) and Arg (LE2) [32]. This aquaammoniaporin signature, which causes a widening of the constriction region that facilitates the transport of both NH_4^+/NH_3, methylammonia and formamide, was also found in the mammalian AQP8 aquaporin [32] and fairly resembles that of NIP-II aquaporins (Ala/Thr (H2), Ile (H5), Ala/Gly (LE1) and Arg (LE2)). Nod26-like aquaporins have been recently demonstrated to transport, in addition to water and glycerol, urea and NH_4^+/NH_3 across the symbiosome membrane [18]. The charged character of the central water channel is of paramount importance for whether attract or repulse ions and thus allow or prevent their transit across the membrane. Typical Nod26-like aquaporins occurring in symbiotic species, e.g. MtNod6, GmNod26, LjLIMP2, PsNod26 and CaNod26, all exhibit a water channel which is electronegatively charged in the extracellular vestibule portion whereas their cytosolic vestibule portion displays a strongly electropositive character (see Figs. 2 and 3). Obviously, this bipartite distribution of electrostatic charges contributes to the attraction or repulsion of ions distributed on both sides of the symbiosome membrane for whether facilitating or hampering their transport across the channel. Moreover, the repulsive effect on NH_4^+ ions of the Arg residue of the ar/R selective filter does not favor its transport by Nod26-like aquaporins. In this respect, Nod26-like aquaporins are more likely to transport the uncharged NH_3 form instead of the charged NH_4^+ ions across the symbiosome membrane. As a comparison, the rat aquaporin AQP8 that had been claimed to transport both the NH_3 and NH_4^+ forms [20], has been recently demonstrated to allow the exclusive transport of NH_3 molecules but preventing NH_4^+ ions from passing the channel [33]. The occurrence of a more widely open ar/R filter (pore size $\geqslant 6$ Å) in both CaNod26 and CpNod26 is compatible with a NH_4^+/NH_3 transport even though its enhanced hydrophilic character is less favorable to the transport of NH_3 due to lower values of the dipole moment (1.49 *vs* 1.85 D for water) and dielectric constant (22 *vs* 80 for water) of liquid NH_3 [32]. Conversely, the widening of the ar/R filter should improve the transport of more bulky and hydrophilic molecules such as urea across biomembranes.

The recent discovery that Nod26-like aquaporins actively participate in the boron uptake by *Arabidopsis* roots [34] and the silicon accumulation in rice (*Oryza sativa*) [11] has shed a new light on the even broader spectrum of transport capacities Nod26-like aquaporins display in higher plants. An Ala residue (Ala132) in the rice transporter Lsi1 involved in silicon uptake seems to be critical since its substitution by a Thr creates a severe clash with Asn108 of the NPA/NPV specific filter. However, the uptake of B and Si by higher plants essentially consists of the bulky boric acid $B(OH)_3$ and silicic acid H_2SiO_3 species that require some widening of the ar/R filter pore to be transported across biomembranes. In this respect, the four residues forming the ar/R filter of the Si transporters in both rice and maize consist of the predominantly hydrophilic and small-sized Ala (H2), Ser (H5), Gly (LE1) and Arg (LE2) residues. This amino acid residue pattern of the ar/R filter closely resembles that of CaNod26 and CpNod26 [Gly (H2), Ser (H5), Gly (LE1), Arg (LE2)] but readily differs from the predominantly hydrophobic and narrower filter [Trp/Ala/Thr (H2), Val/Ile (H5), Ala/Gly (LE1), Arg (LE2)] occurring in other Nod26-like aquaporins of the NIP-I and NIP-II subgroups (Fig. 3). This ar/R filter similarity suggests a possible involvement of CaNod26 and CpNod26 in the Si uptake and translocation in higher plants although they cluster rather far from the rice and maize transporters in the parsimony tree built from the amino acid sequences of the Nod26-like aquaporins.

According to the clustering of Nod26-like aquaporins that supports the close structure-function relationship occurring among these membrane proteins, we propose to identify a new additional NIP-III subgroup for the Nod26-like aquaporins from chickpea (CaNod26) and zucchini (CpNod26) according to their ar/R selective filter that readily differs from other closely-related aquaporins of subgroups NIP-I and NIP-II.

Acknowledgment

The financial support of CNRS is gratefully acknowledged.

References

[1] D. Thomas, P. Bron, G. Ranchy, L. Duchesne, A. Cavalier, J. Rolland, C. Raguenes-Nicol, J. Hubert, W. Haase, C. Delamarche, Aquaglyceroprins, one channel for two molecules, Biochim. Biophys. Acta 1555 (2002) 181–186.

[2] F. Chaumont, F. Barrieu, E. Wojcik, M.J. Chrispeels, R. Jung, Aquaporins constitute a large and highly divergent protein family in maize, Plant Physiol. 125 (2001) 1206–1215.
[3] U. Johanson, M. Karlsson, S. Gustavsson, S. Sjovall, L. Fraysse, A.R. Weig, P. Kjellbom, The complete set of genes encoding major intrinsic proteins in *Arabidopsis* provides a framework for a new nomenclature for major intrinsic proteins in plants, Plant Physiol. 126 (2001) 1358–1369.
[4] F. Quigley, J.M. Rosenberg, Y. Shachar-Hill, H.J. Bohnert, From genome to function: the *Arabidopsis* aquaporins, Genome Biol. 3 (2001) 1–17.
[5] C. Maurel, Plant aquaporins: novel functions and regulation properties, FEBS Lett. 581 (2007) 2227–2236.
[6] M.G. Fortin, N.A. Morrison, D.P. Verma, Nodulin-26, a peribacteroid membrane nodulin is expressed independently of the development of the peribacteroid compartment, Nucleic Acids Res. 15 (1987) 813–824.
[7] J.F. Guenther, D.M. Roberts, Water-selective and multifunctional aquaporins from *Lotus japonicus* nodules, Planta 210 (2000) 741–748.
[8] F. El Yahyaoui, H. Küster, B. Ben Amor, N. Hohnjec, A. Pühler, A. Becker, J. Gouzy, T. Vernié, C. Gough, A. Niebel, L. Godiard, P. Gamas, Expression profiling in *Medicago truncatula* identifies more than 750 genes differentially expressed during nodulation, including many potential regulators of the symbiotic program, Plant Physiol. 136 (2004) 3159–3176.
[9] C.M. Catalano, W.S. Lane, D.J. Sherrier, Biochemical characterization of symbiosome membrane proteins from *Medicago truncatula* root nodules, Electrophoresis 25 (2004) 519–531.
[10] W.-G. Choi, D.M. Roberts, *Arabidopsis* NIP2;1: a major intrinsic protein transporter of lactic acid induced by anoxic stress, J. Biol. Chem. 282 (2007) 24209–24218.
[11] J.F. Ma, K. Tamai, N. Yamaji, N. Mitani, S. Konishi, M. Katsuhara, M. Ishiguro, Y. Murata, M. Yano, A silicon transporter in rice, Nature 440 (2006) 688–691.
[12] I.S. Wallace, D.M. Roberts, Homology modeling of representative subfamilies of *Arabidopsis* major intrinsic proteins. Classification based on the aromatic/arginine selectivity filter, Plant Physiol. 135 (2004) 1059–1068.
[13] R.L. Rivers, R.M. Dean, G. Chandy, J.E. Hall, D.M. Roberts, M.L. Zeidel, Functional analysis of nodulin 26, an aquaporin in soybean root nodule symbiosomes, J. Biol. Chem. 272 (1997) 16256–16261.
[14] S. Biswas, Functional properties of soybean nodulin 26 from a comparative three-dimensional model, FEBS Lett. 558 (2004) 39–44.
[15] I.S. Wallace, W.-G. Choi, D.M. Roberts, The structure, function and regulation of the nodulin 26-like intrinsic protein family of plant aquaglyceroporins, Biochim. Biophys. Acta 1758 (2006) 1165–1175.
[16] A. Arias, G. Martinez-Drets, Glycerol metabolism in *Rhizobium*, Can. J. Microbiol. 22 (2006) 150–153.
[17] L.-J. Ouyang, J. Whelan, D.C. Weaver, D.M. Roberts, D.A. Day, Protein phosphorylation stimulates the rate of malate uptake across the peribacteroid membrane of soybean nodules, FEBS Lett. 293 (1991) 188–190.
[18] C.M. Niemietz, S.D. Tyerman, Channel-mediated permeation of ammonia gas through the peribacteroid membrane of soybean nodules, FEBS Lett. 465 (2000) 110–114.
[19] F. Klebl, M. Wolf, N. Sauer, A defect in the yeast plasma membrane urea transporter Dur3p is complemented by CpNIP1, a Nod26-like protein from zucchini (*Cucurbita pepo* L.), and by *Arabidopsis thaliana* δ-TIP or γ-TIP, FEBS Lett. 547 (2003) 69–74.
[20] L.M. Holm, T.P. Jahn, A.L. Moller, J.K. Schjoerring, D. Ferri, D.A. Klaerke, T. Zeuthen, NH_3 and NH_4^+ permeability in aquaporin-expressing *Xenopus* oocytes, Pflugers Arch. 450 (2005) 415–428.
[21] J.D. Thompson, T.J. Gibson, F. Plewniak, F. Jeanmougin, D.G. Higgins, The CLUSTAL-X windows interface: flexible strategies for multiple sequence alignment aided by quality analysis tool, Nucleic Acids Res. 15 (1997) 4876–4882.
[22] J.-L. Risler, O. Delorme, H. Delacroix, A. Henaut, Amino acid substitutions in structurally related proteins. A pattern recognition approach. Determination of a new and efficient scoring matrix, J. Mol. Biol. 204 (1988) 1019–1029.
[23] C. Gaboriaud, V. Bissery, T. Benchetrit, J.P. Mornon, Hydrophobic cluster analysis: an efficient new way to compare and analyse amino acid sequences, FEBS Lett. 224 (1987) 149–155.
[24] J.K. Lee, D. Kozono, J. Remis, Y. Kitagawa, P. Agre, R.M. Stroud, Structural basis for conductance by the archeal aquaporin AqpM at 1.68 Å, Proc. Natl. Acad. Sci. USA 102 (2005) 18932–18937.
[25] B.L. De Groot, A. Engel, H. Grubmuller, A refined structure of human aquaporin-1, FEBS Lett. 504 (2001) 206–211.
[26] J.W. Ponder, F.M. Richards, Tertiary templates for proteins. Use of packing criteria in the enumeration of allowed sequences for different structural classes, J. Mol. Biol. 193 (1987) 775–791.
[27] M.T. Mas, K.C. Smith, D.L. Yarmush, K. Aisaka, R.M. Fine, Modeling the anti-CEA antibody combining site by homology and conformational search, Proteins Struct. Funct. Genet. 14 (1992) 483–498.
[28] R.A. Laskowski, M.W. MacArthur, D.S. Moss, J.M. Thornton, PROCHECK: a program to check the stereochemistry of protein structures, J. Appl. Crystallogr. 26 (1993) 283–291.
[29] F. Melo, E. Feytmans, Assessing protein structures with a non-local atomic interaction energy, J. Mol. Biol. 277 (1998) 1141–1152.
[30] A. Nicholls, K.A. Sharp, B. Honig, Protein folding and association: Insights from the interfacial and thermodynamic properties of hydrocarbons, Proteins Struct. Funct. Genet. 11 (1991) 281–296.
[31] R.D.M. Page, TREEVIEW: an application to display phylogenetic trees on personal computers, Comput. Appl. Biosci. 12 (1996) 357–358.
[32] T.P. Jahn, A.L.B. Møller, T. Zeuthen, L.M. Holm, D.A. Klærke, B. Mohsin, W. Kühlbrandt, J.K. Schjoerring, Aquaporin homologues in plants and mammals transport ammonia, FEBS Lett. 574 (2004) 31–36.
[33] S.M. Saparov, K. Liu, P. Agre, P. Pohl, Fast and selective ammonia transport by aquaporin-8, J. Biol. Chem. 282 (2007) 5296–5301.
[34] J. Takano, M. Wada, U. Ludewig, G. Schaaf, N. von Wirén, T. Fujiwara, The *Arabidopsis* major intrinsic protein NIP5;1 is essential for efficient boron uptake and plant development under boron limitation, Plant Cell 18 (2006) 1498–1509.